Radiat Environ Biophys (2012) 51:319–329
DOI 10.1007/s00411-012-0416-y

ORIGINAL PAPER

Boron uptake in normal melanocytes and melanoma cells and boron biodistribution study in mice bearing B16F10 melanoma for boron neutron capture therapy

Fernanda Faião-Flores · Paulo Rogério Pinto Coelho · João Dias Toledo Arruda-Neto · Maria Aparecida Pires Camillo · Silvya Stuchi Maria-Engler · Rose Eli Grassi Rici · Jorge Eduardo Souza Sarkis · Durvanei Augusto Maria

Received: 17 November 2011 / Accepted: 31 March 2012 / Published online: 11 April 2012

Abstract Information on ^{10}B distribution in normal tissues is crucial to any further development of boron neutron capture therapy (BNCT). The goal of this study was to investigate the in vitro and in vivo boron biodistribution in B16F10 murine melanoma and normal tissues as a model for human melanoma treatment by a simple and rapid colorimetric method, which was validated by HR-ICP-MS. The B16F10 melanoma cell line showed higher melanin content than human melanocytes, demonstrating a greater potential for boronophenylalanine uptake. The melanocytes showed a moderate viability decrease in the first few minutes after BNCT application, stabilizing after 75 min, whereas the B16F10 melanoma showed the greatest intracellular boron concentration at 150 min after application, indicating a different boron uptake of melanoma cells compared to normal melanocytes. Moreover, at this time, the increase in boron uptake in melanoma cells was approximately 1.6 times higher than that in normal melanocytes. The ^{10}B concentration in the blood of mice bearing B16F10 melanoma increased until 90 min after BNCT application and then decreased after 120 min, and remained low until the 240th minute. On the other hand, the ^{10}B concentration in tumors was increased from 90 min and maximal at 150 min after application, thus confirming the in vitro results. Therefore, the present in vitro and in vivo study of ^{10}B uptake in normal and tumor cells revealed important data that could enable BNCT to be possibly used as a treatment for melanoma, a chemoresistant cancer associated with high mortality.

Keywords Boron neutron capture therapy · 10B measurement · Boronophenylalanine · B16F10 melanoma · C57Bl/6J mice

F. Faião-Flores (✉) · D. A. Maria (✉)
Laboratory of Biochemistry and Biophysics, Butantan Institute, 1500 Vital Brasil Avenue, São Paulo, SP 05503-900, Brazil
e-mail: fernandafaiao@usp.br

D. A. Maria
e-mail: durvanei@usp.br

F. Faião-Flores
Faculty of Medicine, University of São Paulo, São Paulo, SP, Brazil

P. R. P. Coelho · M. A. P. Camillo · J. E. S. Sarkis
Institute for Nuclear and Energy Research, São Paulo, SP, Brazil

J. D. T. Arruda-Neto
Physics Institute, University of São Paulo, São Paulo, SP, Brazil

J. D. T. Arruda-Neto
CEPESq/UniÍtalo—Italy-Brazilian University Center, São Paulo, SP, Brazil

S. S. Maria-Engler
Department of Clinical Chemistry and Toxicology, School of Pharmaceutical Sciences, University of São Paulo, São Paulo, SP, Brazil

R. E. G. Rici
Faculty of the Veterinary Medicine and Zootechny, Department of Surgery, University of São Paulo, São Paulo, SP, Brazil

Introduction

Melanoma, a highly invasive and metastatic tumor type, has shown an increasing incidence and mortality in recent years (Jemal et al. 2009). It is the most aggressive skin cancer and causes the majority of deaths among skin cancer cases (Mendes et al. 2008). Melanoma is currently being cured by surgical excision if detected early. However, melanoma with distant metastasis is still incurable (Larrosa et al. 2003).

Boron neutron capture therapy (BNCT) is a binary treatment modality involving the selective accumulation of

^{10}B carriers in tumors followed by irradiation with a thermal or epithermal neutron beam (Trivillin et al. 2008). High linear energy transfer (LET) alpha particles and recoiling ^{7}Li nuclei are emitted during the capture of thermal neutrons by ^{10}B nuclei and deposit their energy with a high relative biological effectiveness in biological material (Coderre and Morris 1999).

The basic idea of BNCT is that if ^{10}B is taken up selectively by tumor tissue, then capture reactions will occur preferentially in tumor cells, and the resulting high LET particles will travel only a very short distance (corresponding roughly to the size of a cell/cell nucleus) (Trivillin et al. 2008). BNCT would, thus, potentially target neoplastic tissue selectively (Coderre et al. 1990).

Neutron irradiations should be performed at the point in time after the boron compound is administered, when there is both a high absolute boron concentration in the tumor and high tumor/normal tissue and tumor/blood ratios (Kreimann et al. 2003). Clinical trials of BNCT for the treatment of melanoma using L-*para*-boronophenylalanine (BPA) as the boron compound have been performed (Fukuda et al. 1994; Menéndez et al. 2009) and are currently in progress in Finland, Sweden, Japan, Argentina, Italia and others. Experimental studies have been carried out employing a variety of experimental models based on the implantation of tumor cells in normal tissue (Barth et al. 1994; Coderre et al. 1991).

Despite numerous investigations, inconclusive information is available regarding ^{10}B metabolism and uptake in normal tissues. Note that information on the ^{10}B distribution in normal tissues is crucial for any further development of BNCT in a broadened spectrum of indications where the dose delivered to normal tissue is a limiting factor for the therapy. In-depth knowledge on the boron bioavailability in normal tissues may offer another starting point for treatment optimization, because it is an important parameter that influences normal tissue injury (Wittig et al. 2009). Cho and coworkers already showed a BPA biodistribution in C57BL/6J mice bearing B16F10 melanoma by prompt gamma analysis (Cho et al. 2007). However, their study included only few data about the curve for BPA biodistribution in this melanoma model, and there was no determination of the best time for BPA administration before thermal neutron irradiation.

In this study, the boron biodistribution in B16F10 murine melanoma and normal tissues as a model for human melanoma treatment with BNCT was investigated in detail.

Materials and methods

Cell lines

A tumor cell line of murine melanoma (B16F10) was cultivated in 75-cm^2 flasks with RPMI-1640 (Cultilab) medium supplemented with 10 % inactive fetal bovine serum (Cultilab), 2 mM of L-glutamine (Sigma Chemical Company) and 0.1 mg/mL streptomycin (FontouraWyeth AS). A human primary culture of melanocytes isolated from foreskin was cultivated with 254CF medium (Life Sciences®) supplemented with 10 % inactive fetal bovine serum HMGS (Life Sciences®) and 0.1 mg/mL streptomycin (FontouraWyeth AS), as previously described (Fernandez et al. 2005). Cell suspensions were obtained from adherent cells by a 5-min treatment with trypsin 0.2 % and subsequent inactivation of trypsin with 10 % fetal bovine serum (FBS)–enriched medium. The nonadherent cells were centrifuged twice, resuspended in medium, then seeded in plates and allowed to grow for 24 h.

Boronophenylalanine (BPA)

^{10}B-enriched (> 99 %) BPA (molecular weight = 209.01 g) was purchased from KatChem and converted to a fructose 1:1 complex to increase its solubility (Coderre et al. 1994).

Melanin content assay

The content of melanin was determined according to the procedure described by Meyskens (Meyskens 1981) and modified by Zhao (Zhao et al. 2003). Melanocytes and B16F10 melanoma cells were plated in different flasks containing 10 mL of RPMI 1640 medium. After 24 h, each cell type was removed from the dish by 0.25 % trypsin, and the cells were counted and adjusted to a concentration of 10^3 cells/mL. After centrifugation for 10 min, the cells were washed twice with phosphate-buffered saline (pH 7.0), and 10^3 cells were dissolved in 1.0 mL of 1 N NaOH and 10 % dimethyl sulfoxide for 30 min. Thereafter, the absorbance at 470 nm was recorded.

Cell treatment and BNCT irradiation

Melanocytes and B16F10 melanoma cells were seeded in 96-well plates at a concentration of 10^5 cells/mL and allowed to grow for 24 h. They were then treated with BPA at a concentration of 4.18 mg/mL, corresponding to 220 μg ^{10}B/mL. After different incubation time intervals (from 15 to 180 min), the cells were irradiated at the BNCT research facility of the Nuclear and Energetic Research Institute (IPEN, Brazil) (Coelho et al. 2002) for a period of 10 min, using the IEA-R1 nuclear reactor operating at a power of 3.5 MW. The thermal neutron flux, epithermal neutron flux and fast neutron flux at the irradiation position were $(2.31 \pm 0.03) \times 10^8$, $(4.60 \pm 0.10) \times 10^6$ and $(3.50 \pm 0.10) \times 10^7$ n/cm^{2}s, respectively. The gamma dose rate in air at the irradiation site was 3.50 ± 0.80 Gy. Before

irradiation, the BPA-enriched incubation medium was removed, and the cells were washed in 0.9 % saline solution. A sample that was not irradiated or treated with BPA was also studied, representing the "control group" (time 0). Images of the control and treated cells were taken using a camera (Sony Cyber-shot 7.2 megapixels) coupled to an optic inverted microscope (Carl Zeiss), magnified at 40 × . Another cell group was irradiated without BPA (beam only) and was termed the "irradiated control."

Cellular viability assay—MTT

The cellular viability of B16F10 melanoma and melanocytes treated with BNCT was determined using colorimetric methodology, MTT (3-(4,5-dimethylthiazol-2-yl)2,5-diphenyl tetrazolium bromide) (Sigma), which is based on MTT reduction of formazan by living cells (Mosmann 1983). MTT is reduced in metabolically active cells to form insoluble purple formazan crystals, which are solubilized by the addition of a detergent. The color is then quantified by spectrophotometric means. For each cell type, a linear relationship between cell number and absorbance is established, enabling accurate, straightforward quantification of changes in proliferation. This colorimetric assay is well established; it is widely used and described in several papers (Kamida et al. 2008).

Cell treatment for boron concentration analysis

Melanocytes and B16F10 melanoma cells were seeded in dishes at a concentration of 10^6 cells/mL and were allowed to grow for 24 h. After this period, they were treated with BPA at a concentration of 4.18 mg/mL, corresponding to 220 μg ^{10}B/mL. The medium was then collected at times ranging from 0 to 180 min, and the cells were removed from the dish with 0.25 % trypsin. These samples were stored at −20 °C until later analysis.

In vivo biodistribution for boron concentration analysis

All animal experiments were carried out according to the regulations of the Ethical Committee for Animal Research at the Butantan Institute (479/09). C57Bl/6J female mice (18–23 g) were divided into ten groups of five mice each. The animals were maintained with diet and water ad libitum. The B16F10 melanoma cells (10^4/0.1 mL of culture medium) were inoculated subcutaneously in the dorsal skin of C57Bl/6J mice. Forty days after inoculation with tumor cells, the mice received BPA (750 mg/kg body mass intraperitoneally (i.p.). Samples were taken from 0 to 240 min after BPA administration (for colorimetric assay). Blood samples were drawn from submandibular vein. The mice were euthanized by cervical dislocation and then necropsied. The following samples were excised: tumor, adjacent normal skin (0.1 cm^2), and several organs such as liver, kidney, intestine, spleen, brain, heart and lung after different time periods.

Sample preparation by boron concentration analysis

Tissue samples were taken, cleaned out from blood with saline solution, weighed and digested by 1:1 HNO_3 and H_2O_2 solutions. All samples were exposed to ultrasound for 60 min at 80 °C.

Boron concentration analysis by colorimetric method

The samples were placed inside quartz tubes with 1 mL of water and 0.5 mL of 2 % (w/v) aqueous solution of $KMnO_4$. The mixture was incubated for 1 h at 95 °C and then cooled to room temperature. The samples were then treated with 2 mL of 10% (v/v) 2-ethyl-1,3-hexanediol in $CHCl_3$ and shaked for 3 min. The aqueous phase containing precipitated MnO_2 was removed by aspiration. An aqueous solution of curcumin (1.0 mL) and 0.3 mL of H_2SO_4 were then added to 0.5 mL of $CHCl_3$ extract. The mixture was allowed to stand for 15 min at room temperature, and then, 50 mL of 95 % (v/v) EtOH was added. The color of this solution, ranging from orange-yellow to red, reveals the amount of boron present (Ikeuchi and Amano 1978). The absorbance at 555 nm was read using a Thermo Scientific Genesys 6® spectrophotometer. The calibration curve was linear from 0.2 to 440 μg of boron in the BPA standard solution.

Boron concentration analysis by high resolution inductively coupled plasma mass spectrometry (HR-ICP-MS) technique

To confirm and validate the results from boron concentration analysis by colorimetric assay, some samples were sorted out for boron concentration analysis by HR-ICP-MS. These samples corresponded to 0 min (mice bearing B16F10 melanoma tumor without BPA injection—control group) and BPA post-injection time of 150 min.

All HR-ICP-MS measurements were taken in a HR-ICP–MS (Element 1, Thermo Finnigan MAT GmbH, Bremen, Germany). The Element 1 is equipped with a self-aspirating microconcentric nebulizer, a Scott-type spray chamber, a Fassel torch and a 27-MHz generator. Instrumental settings and optimized measurement parameters for boron isotopes are given in Table 1. Isotopic measurements were taken using only electric scanning (E-scanning) and at a medium-resolution setting (R = 3,500).

Table 1 HR-ICP-MS instrument settings and scanning conditions

Sample introduction system and instrumental operating conditions	
Nebulizer (mL/min)	1
Spray chamber	Scott-spray chamber
Sampling cone	Nickel
Skimmer cone	Nickel
RF power (W)	1,200
Plasma gas flow rate (L/min)	16
Auxiliary gas flow rate (L/min)	0.9
Nebulizer gas flow rate (L/min)	1
Measurement conditions	
Resolution (10 % valley definition)	Medium, $M/\Delta M = 3{,}500$
Acquisition mode	E-scan
Magnet setting time (s)	0.001
Mass range (amu)	
^{10}B	10.010–10.012
^{11}B	11.006–11.012
Search window (%)	120
Integration window (%)	60
Sample time (s)	0.02
Numbers of channels per peak	30
Segment duration (s)	2
Detection mode	Ion counting
Number of replicates	15
Dead time correction (ns)	10

Scanning electron microscopy

B16F10 cells and melanocytes (at 150 min, the time point corresponding to the main reduction in B16F10 viability) were rinsed with phosphate-buffered saline (PBS) twice and fixed with 3 % glutaraldehyde in PBS incubating overnight at room temperature. After washing with PBS thrice again, the samples were fixed with 1 % osmium tetroxide (pH 7.4) at 4 °C for 1 h. The samples were dehydrated, dried in a critical point drier and gold sputtered. Scanning electron microscopic (SEM) images were then taken on a LEO 453 VP, Electron Microscopy.

Statistical analysis

The data were analyzed using the unpaired t test, followed by Welch's *t* test with *p* values less than 0.0001 considered extremely significant. These analysis methods were used to compare the melanin synthesis between the two cell types.

Results

In vitro selective boron uptake

Both cell types were subjected to boron quantification analysis. A standard curve was obtained using BPA, and an analysis method in tissues and cells was developed (Fig. 1). In the boron concentration analysis, the uptake in melanocytes was similar in the first minutes of incubation (15–60 min). From 75 min onward, the same intracellular boron concentration was maintained in the melanocytes (Fig. 2a), whereas the B16F10 melanoma cells were observed to show an increased boron uptake at the same time (Fig. 2b). The greatest intracellular boron concentration in tumor cells was obtained at 150 min, showing boron uptake selectivity greater in B16F10 melanoma cells when compared to normal melanocytes. Moreover, at 150 min, there was roughly 160 μg per 10^6 cells of boron uptake in B16F10 melanoma cells, whereas the highest boron uptake by melanocytes was only 100 μg per 10^6 cells at 60 min of incubation (an approximate increase of 1.6 times). In melanoma cells, there is an increase in boron uptake; therefore, there is a decrease in boron in supernatant. In contrast, in melanocytes cells, there is not much uptake, so there is a constant boron concentration in supernatant.

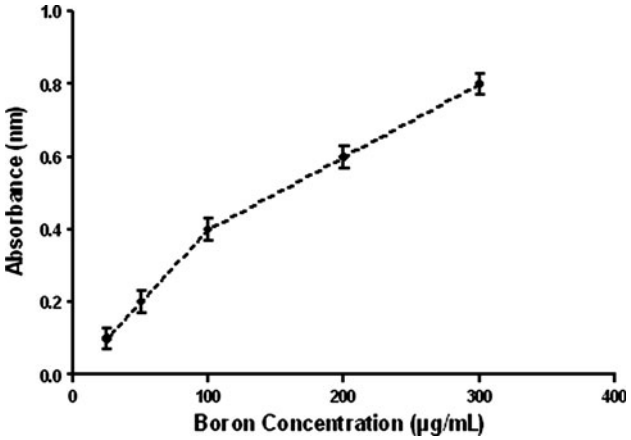

Fig. 1 Standard curve used for boron concentration determination in melanocytes and melanoma cells and tissues of mice bearing B16F10 melanoma

Increased cytotoxicity and higher melanin production in B16F10 melanoma cells

Upon confirming the boron uptake data in both cell types, melanocytes showed a viability decrease in the first minutes (15 min) and then an increase from 15 min onward, keeping a constant increase rate up to 180 min. In contrast, melanoma cells exhibited a stable viability decrease (between 15 and 135 min), with a cytotoxicity peak at 150 min (viability decline of approximately 40 %). There was a steady increase from this point on, indicating boron elimination with a consequent reduction in BNCT effectiveness (Fig. 3a). The irradiated control group did not show any significant differences compared to the control group (without BPA and without irradiation).

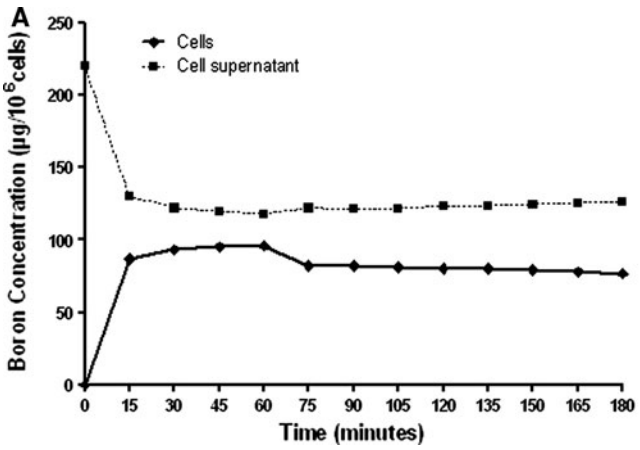

Fig. 2 Boron concentration in melanocytes and melanoma cells. **a** Boron concentration in melanocytes with BPA incubation from 0 to 180 min in cells and cell supernatants. **b** Boron concentration in melanoma with BPA incubation from 0 to 180 min in cells and cell supernatants. *Each point* represents mean ± standard deviation of the results from three experiments performed in triplicate

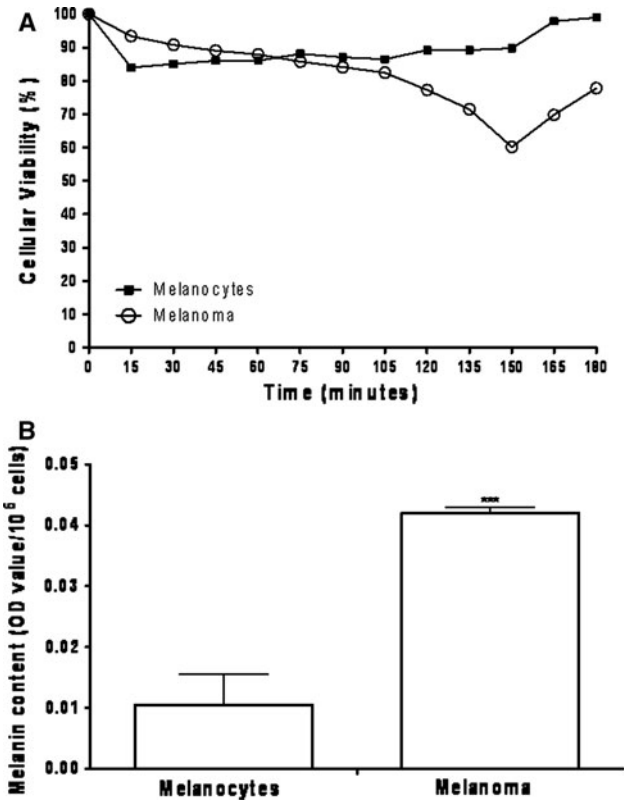

Fig. 3 **a** Melanocytes and melanoma cell viability after BPA incubation from 0 to 180 min and thermal neutron irradiation. **b** Melanin content in melanocytes and melanoma cells. Each point represents mean ± standard deviation of the results from three experiments performed in triplicate

These differences in boron uptake with a consequent reduction in the viability of the tumor cells could be related to the amount of melanin produced by B16F10 melanoma cells, which showed approximately four times more melanin synthesis compared to normal melanocytes (Fig. 3b).

These results were confirmed by analysis of morphological changes of the cell population distribution in each time period (Fig. 4). Melanocytes were observed to have some debris and had a density population similar to the control group for all times. However, B16F10 melanoma cells had a viability decrease, with a sharp peak at 150 min, as it is observed in Fig. 3a, thus confirming the MTT results and indicating that cells with more melanin are more affected by BNCT.

Cells analysis using scanning electron microscopy in the best period of BNCT application

After 150 min, the B16F10 melanoma cells showed the greatest decrease in cell viability, indicating the best point of administration of BPA followed by irradiation with thermal neutrons. At this time point, images were taken using scanning electron microscopy of these cells and the normal melanocytes cell line to make a comparison. It can be observed that the B16F10 melanoma cells in the control group (Fig. 5a) were intact, with the preservation of normal cell contours and the presence of mitotic figures. In contrast, B16F10 melanoma cells treated with BNCT (Fig. 5b) showed apoptotic bodies with degradation of the extracellular matrix. Melanocytes in the control group (Fig. 5c) showed the cytoplasmic morphology characteristic of this cell line, without the presence of cytoplasmic vacuolization. Melanocytes treated with BNCT (Fig. 5d) also showed preserved normal cell limits with few cellular changes. Thus, it can be concluded that the best period for irradiation with thermal neutrons is after 150 min of BPA incubation, to have the most deleterious effect on melanoma cells, with minimal side effects in normal cells.

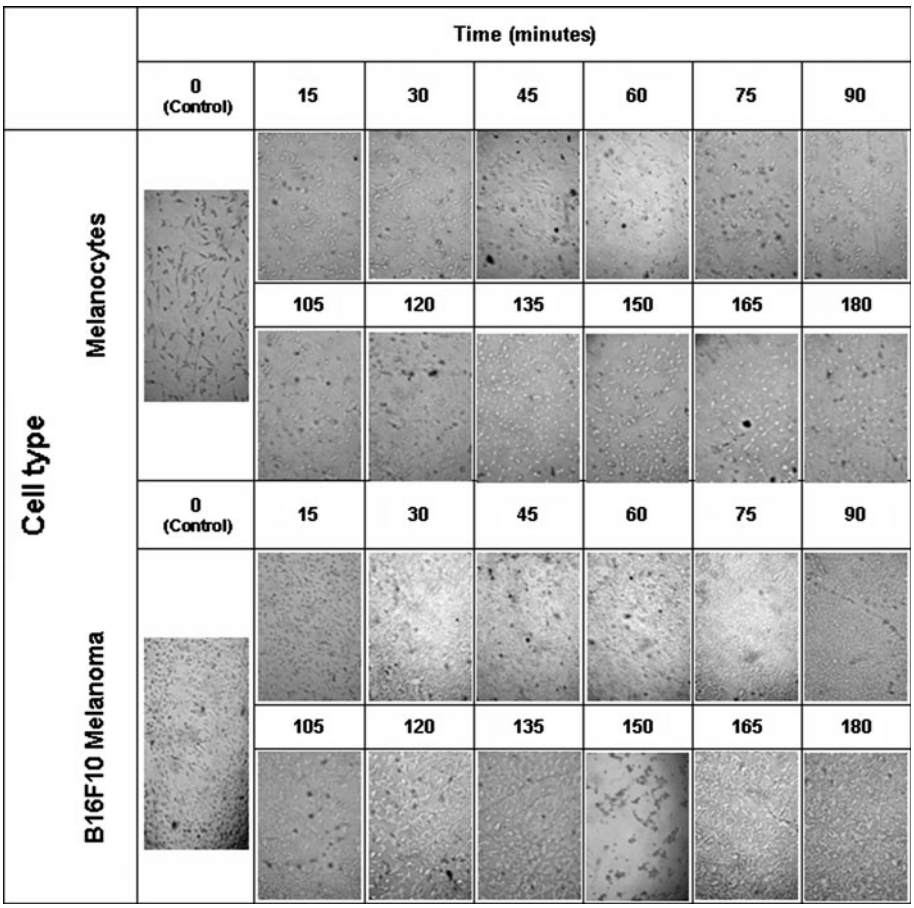

Fig. 4 Photomicrographs of melanocytes and melanoma cells after BPA incubation from 0 to 180 min and thermal neutron irradiation corresponding to Fig. 2a. Images of the control and treated cells were taken by a camera (Sony Cyber-shot 7.2 mega pixels) coupled to an optic inverted microscope (Carl Zeiss), magnified at 40×

In vivo boron biodistribution

To analyze the boron concentration within organs, tumors and blood, we used the standard curve (Fig. 1), with boron concentrations ranging from 0 to 300 μg/mL of selected samples. During the first minutes after BPA administration, a significant increase in the boron concentration in blood (between 15 and 90 min) was observed, followed by a sharp drop at 120 min. At 90 min and later, a high intratumoral boron concentration increase was observed, peaking after 150 min at approximately 100 ppm. A small amount of boron (approximately 35 μg per 10^6 cells) in the tumor, with no significant amount observed in the blood, was also found in the last measured period (Fig. 6a). In terms of the ratio between the amount of boron in blood and in the tumor, after 150 min of BPA administration, which is quite adequate for this type of treatment, there was approximately 10 times more boron in the tumor than in blood (Fig. 6b).

Boron biodistribution in other organs was also studied, indicating that liver, heart and lung do not take up boron from BPA. Other organs such as spleen and brain captured minimal quantities of this element compound (Table 2). Additionally, there was an increase in boron in the kidney after 210 min and in the intestine after 240 min due to its clearance. Another relevant finding was the low boron uptake in normal skin adjacent to the tumor, indicating a higher uptake by B16F10 melanoma cells.

Validation of the colorimetric method by comparison with HR-ICP-MS

The mice of the control group (time 0) and mice that received BPA 150 min before euthanasia were analyzed, in order to compare the colorimetric and HR-ICP-MS methods. All values obtained by the colorimetric method were consistent with those obtained by HR-ICP-MS (Table 3); that is, differences were within the error bars of both methods. Therefore, the colorimetric method was validated.

Discussion

Malignant melanoma is the most aggressive form of cancer, causing the majority of deaths among skin cancers. Although representing less than 10 % of skin cancers, it is responsible for more than 75 % of skin cancer-related

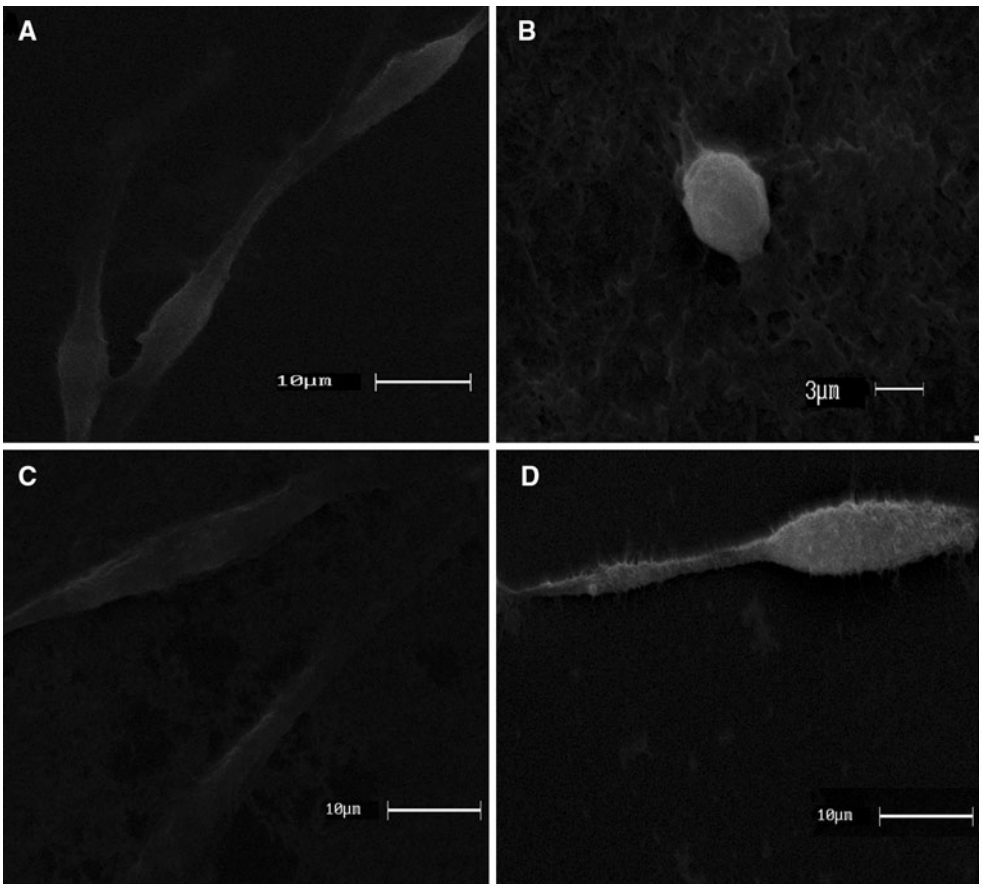

Fig. 5 Photomicrographs of scanning electron microscopy of B16F10 melanoma cells and melanocytes. **a** Cells from the control group of B16F10 melanoma cells. **b** B16F10 melanoma cells treated with thermal neutrons at 150 min after BPA incubation. **c** Normal melanocytes of the control group. **d** Normal melanocytes treated with thermal neutrons at 150 min after BPA incubation

deaths. The notorious resistance of malignant melanoma to all current chemotherapeutic regimens remains a major obstacle for its successful treatment (Gogas et al. 2009). Common treatments for malignant melanoma involve a combination of therapies including surgical removal, chemotherapy and radiotherapy. However, the reported five-year survival rate of melanoma is still discouraging due to its chemoresistance and metastasis. In particular, the most commonly utilized chemotherapeutic regimens have been tried without significantly increasing overall survival rates among metastatic melanoma patients (Jiang et al. 2010).

The next step in optimizing radiotherapy might be achieved by targeting the radiation in a way that, in principle, it is able to selectively kill tumor cells while sparing the surrounding normal tissues. One such treatment option may be BNCT, which, because of the limited spatial distribution of its effects, produces a highly selective delivery of radiation (Wittig et al. 2009). Therefore, if ^{10}B can be delivered selectively to tumor cells, then the short range of the charged particles produced in BNCT would offer the potential for targeting radiation to individual tumor cells with high biological efficacy (Coderre and Morris 1999; Sauerwein 1993; Barth 2003; Yamamoto et al. 2008).

In BNCT, a flux of neutrons of appropriate energy is set to react with ^{10}B isotopes that have accumulated in tumor cells. Selective accumulation is achieved by administering BPA enriched in ^{10}B. This step is followed by bombardment with a thermal neutron beam, generated in a nuclear reactor, which induces an (n, α) reaction with ^{7}Li and ^{4}He (α-particle) as products. As the mean free paths of both particles are of the same order as the size of the tumor cells, these are destroyed without the normal tissue suffering any significant damage (Gautier et al. 2007).

A comprehensive review of the methods for analysis of clinical and biological samples for boron has been provided (Probst 1999), and the colorimetric assay for boron concentration analysis is favored because it is a simple and quick method for quantifying boron in the samples to be used for BNCT.

The B16F10 cells may offer an approach to investigate the properties of malignant cells. This cell line has been studied since 1975 and has reliable characteristics that are

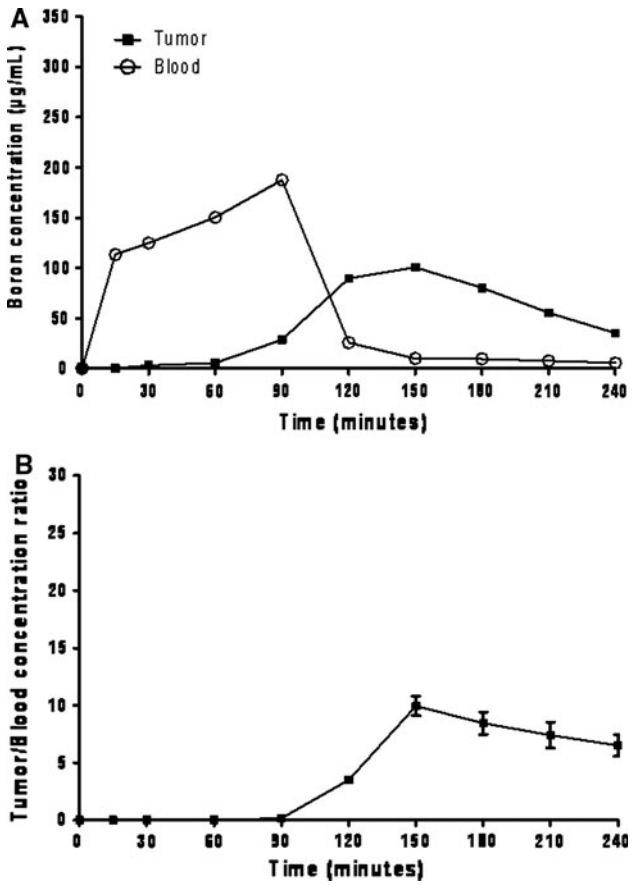

Fig. 6 In vivo boron concentrations in tumor, blood and normal tissues. **a** Boron concentration in tumor and blood after BPA administration from 0 to 240 min. **b** Tumor/blood concentration ratio of boron after BPA administration from 0 to 240 min. Each point represents mean ± standard deviation of the results from three experiments performed in triplicate

similar to human melanomas (Fidler 1975). Thus, this model has been chosen here to study the in vitro ^{10}B uptake and the in vivo uptake model in C57Bl/6J mice.

BPA is an analog of an essential amino acid phenylalanine and is actively taken up in cells not only as an amino acid analog for protein synthesis, but also as a tyrosine analog for melanogenesis. Due to these properties, BPA has been clinically utilized for malignant melanoma (Mishima et al. 1989). The B16F10 melanoma cell line showed approximately four times more melanin than normal melanocytes (Fig. 3b), demonstrating a greater potential for BPA uptake (Fig. 2b) in comparison with the lower ^{10}B uptake by normal melanocytes (Fig. 2a). In B16F10 cells, the BPA uptake increased after 75 min of incubation.

The analysis of the boron content in the supernatant is also important for confirming the amount of boron uptake as function of time (Probst 1999). For instance, the results in Fig. 2 indicate that the amount of ^{10}B decreases in the

Table 2 Boron concentration in tumor, blood and normal tissues after BPA administration from 0–240 min (μg per 10^6 cells)

Tissues	Time (min)										
	0	15	30	60	90	120	150	180	210	240
Liver	0.1 ± 0.1	0.1 ± 0.0	0.1 ± 0.0	0.1 ± 0.0	0.1 ± 0.0	0.1 ± 0.0	0.1 ± 0.0	0.1 ± 0.0	0.1 ± 0.0	0.1 ± 0.0
Kidney	9.2 ± 0.1	9.2 ± 0.1	10.1 ± 0.2	12.9 ± 0.1	12.9 ± 0.2	12.8 ± 0.2	13.2 ± 0.3	13.4 ± 0.3	27.8 ± 1.0	30.3 ± 2.3
Intestine	0.7 ± 0.1	0.7 ± 0.1	0.7 ± 0.1	0.7 ± 0.1	0.7 ± 0.1	0.7 ± 0.1	0.9 ± 0.4	1.1 ± 0.3	8.9 ± 1.2	19.2 ± 2.4
Skin	3.5 ± 0.5	3.5 ± 0.4	3.7 ± 0.4	3.8 ± 0.3	4.3 ± 0.9	4.9 ± 1.1	4.8 ± 1.2	4.7 ± 0.9	4.2 ± 0.8	4.1 ± 0.9
Spleen	0.7 ± 0.2	0.7 ± 0.1	2.5 ± 0.3	5.6 ± 1.0	6.3 ± 1.2	7.8 ± 1.4	8.1 ± 1.2	8.4 ± 1.5	7.5 ± 1.1	7.2 ± 0.9
Brain	1.3 ± 0.2	1.3 ± 0.1	1.3 ± 0.2	2.9 ± 04	3.0 ± 0.9	3.1 ± 0.8	3.5 ± 1.0	7.5 ± 1.5	6.5 ± 1.4	6.0 ± 0.9
Heart	0.1 ± 0.1	0.1 ± 0.0	0.1 ± 0.0	0.1 ± 0.0	0.1 ± 0.0	0.1 ± 0.0	0.1 ± 0.0	0.1 ± 0.0	0.1 ± 0.0	0.1 ± 0.0
Lung	0.1 ± 0.1	0.1 ± 0.0	0.1 ± 0.0	0.1 ± 0.0	0.1 ± 0.0	0.1 ± 0.0	0.1 ± 0.0	0.1 ± 0.0	0.1 ± 0.0	0.1 ± 0.0
Blood	2.1 ± 0.1	113.2 ± 8.1	124.9 ± 12.2	150.4 ± 15.1	187.7 ± 12.2	25.6 ± 5.9	10.1 ± 1.4	9.5 ± 1.9	7.5 ± 1.1	5.3 ± 0.9
Tumor	0.2 ± 0.1	0.2 ± 0.0	3.0 ± 0.4	5.3 ± 1.7	28.6 ± 2.4	89.5 ± 3.5	100.5 ± 15.1	80.2 ± 9.5	55.5 ± 8.4	35.2 ± 5.9

Table 3 Boron concentration comparison between colorimetric method and ICP-MS method at 0 (control) and 150 min after BPA administration

Tissue	Boron concentration analysis (μg per 10^6 cells)			
	Colorimetric method		ICP-MS method	
	0 (control)	150 min	0 (control)	150 min
Liver	0.1 ± 0.1	0.1 ± 0.1	0.3 ± 0.1	0.3 ± 0.1
Kidney	9.2 ± 0.1	13.2 ± 0.3	9.5 ± 0.9	12.3 ± 1.2
Intestine	0.7 ± 0.1	0.9 ± 0.4	0.7 ± 0.1	1.4 ± 0.3
Skin	3.5 ± 0.5	4.8 ± 1.2	3.2 ± 0.1	4.2 ± 0.4
Spleen	0.7 ± 0.2	8.1 ± 1.2	0.3 ± 0.2	6.2 ± 0.6
Brain	1.3 ± 0.2	3.5 ± 1.0	1.0 ± 0.1	4.2 ± 0.4
Heart	0.1 ± 0.1	0.1 ± 0.1	0.3 ± 0.1	0.3 ± 0.1
Lung	0.1 ± 0.1	0.1 ± 0.1	0.2 ± 0.1	0.3 ± 0.1
Blood	2.1 ± 0.1	10.1 ± 1.4	2.4 ± 0.2	10.6 ± 1.6
Tumor	0.2 ± 0.1	100.5 ± 15.1	0.6 ± 0.3	80.4 ± 8.1

supernatant, while there is an increase within the cells, as shown in panels a and b. This finding corroborates with the cell viability shown in Fig. 3a. Furthermore, probably there was no boron reabsorption by melanocytes and B16F10 melanoma cells because there was no increase in boron amount after the peak concentration during the evaluated time.

The data shown in Fig. 2 were confirmed since there is an accentuated drop in melanoma cells viability, falling to a minimum at 150 min after BPA incubation (Fig. 3a). The melanocytes viability moderately decreased in the first minutes, but the cell viability trend was stable and nearly constant from 45 min onward. These results are consistent with those presented in Fig. 4, where a decreased confluence and debris formation in melanoma cells over time is observed, whereas there are no significant differences between melanocytes incubated with BPA and cells from the control group. These findings in B16F10 melanoma cells can confirm the inhibition of cell proliferation by a decrease in cyclin D1, with apoptosis by DNA fragmentation (Faião-Flores et al. 2011a) and cell death mainly occurring in the tumor cells as a result of free radical production (Faião-Flores et al. 2011b). The results of the present study are consistent with those obtained in these previous studies. Results of previous studies obtained by our group (Faião-Flores et al. 2011b) that included the irradiated control under the same conditions have already been published. In the present paper, we did not find—same as in Faião-Flores et al. 2011b—any significant difference between the irradiated control and the control group.

Boron compounds for BNCT do not themselves have any therapeutic effect, and the methods used to measure the ^{10}B concentration in tissue are generally invasive. Thus, the number of patients who can be included in trials examining only the uptake of compounds in tissue is very limited (Wittig et al. 2008a, b). Consequently, animal studies play a central role in characterizing the bioavailability of compounds for the rational design of future BNCT trials.

Some articles have reported on the boron biodistribution in various models, for example, melanoma in hamsters (Ichikawa et al. 2009), undifferentiated thyroid carcinoma in mice (Dagrosa et al. 2005) and Walker 256 tumors in rats (Suzuki et al. 2004). However, there are no detailed studies about BPA biodistribution as a function of time by intraperitoneal inoculation in B16F10 murine melanoma, which is widely used and reflects the metastatic potential of melanoma.

BPA administration in mice bearing B16F10 melanoma showed significant results in terms of ^{10}B capture in tumor tissue. The ^{10}B concentration in blood rose up to 90 min after administration and fell thereafter, maintaining low values until a time of 240 min after administration. On the other hand, the ^{10}B concentration in the tumor increased from 60 min onward, reaching a maximum at 150 min, thus confirming the in vitro results. However, the maximum ^{10}B concentration in the tumor decreased more significantly from 180 min onward (Fig. 6a).

To achieve therapeutically appropriate pharmacokinetics in BNCT, a tumor/blood boron concentration ratio of at least greater than one must be achieved, meaning that the boron compound should accumulate and persist within the tumor cells, while the blood concentrations decrease (Soloway et al. 1998). We observed that the tumor/blood concentration ratio increased from 90 min onward, with a peak at 150 min, corresponding to a tumor/blood concentration ratio, which is approximately 10 (Fig. 6b). A minimum tumor boron concentration of approximately 20 μg per 10^6 cells and a tumor/blood concentration ratio of at least 3:1 have been established as requirements for the potential success of the procedure (Dagrosa et al. 2005). These requirements are met here between 120 and 240 min

after administration. In the present study, although the tumor/blood concentration ratio was higher than 3:1, the tumor/healthy tissue dose ratio depends on other factors, as the gamma fluence at the irradiation place.

For BNCT, a sufficient number of ^{10}B atoms must accumulate in the tumor, and the gradient of the amount of ^{10}B atoms between the tumor and the surrounding normal tissues must be large (Suzuki et al. 2004). Interestingly, the concentrations of boron in B16F10 melanoma cells and B16F10 tumors in mice were higher than those reported in the literature. This finding may be related to two main hypotheses: (1) the B16F10 cell line shows a higher melanin content compared to other melanoma cell lines (Fidler 1975) and (2) BPA uptake could occur through the L-type amino acid transporter 1 (LAT 1) that helps to capture BPA because of the phenylalanine that is present in the BPA molecule and that is required by cells during intense proliferative activity (Uchino et al. 2002).

Some organs such as the liver, heart and lungs did not show increased ^{10}B uptake, while spleen and normal skin displayed moderate increases. The kidney and intestine showed a moderate ^{10}B increase from 210 min after administration onward, indicating clearance of the compound. The quantification of ^{10}B in organs such as the spleen and liver is important for evaluating BPA metabolism, and kidney and intestine are relevant for excretion analysis (Probst 1999). The absolute mean ^{10}B concentrations in tumor, normal tissues and blood are summarized in Table 1.

The HR-ICP-MS method also used in the present study is applicable for boron to be measured at ppb levels in serum, plasma, urine, plants, saline, water and tissue (Wittig et al. 2008a, b; Mattiello et al. 2011). It was used here to validate results of boron concentration analysis by the colorimetric method. The control group (time 0) and mice that received BPA 150 min before analysis were used to validate all samples. All results were found compatible with both methods by comparing the medians with the standard deviations (SD). In this way, the colorimetric method can be used to facilitate boron concentration analysis in tissue samples.

Conclusions

Biodistribution of the administered ^{10}B compounds in vivo is among the many problems to be solved before a successful clinical implementation of BNCT. Understanding how the ^{10}B compounds are absorbed and distributed is crucial for correctly calculating the beginning of irradiation. The ideal irradiation time is when the tumor/blood concentration ratio is maximal, while the boron concentration near the tumor cells is minimal. In summary, it was shown here the best time period for thermal neutron irradiation to be 150 min after BPA incubation for metastatic melanoma treatment, represented here by the B16F10 melanoma model. It was at this time that the highest ^{10}B concentration in tumor cells in vitro and in the in vivo melanoma model was observed.

Thus, in vitro and in vivo studies of ^{10}B uptake in normal and tumor cells can provide important data that can help lead to successful BNCT application under the best possible conditions for many cancer types. These cancers include those with a high mortality rate such as melanoma. BNCT can be used as an important tool in human melanoma treatment with high effectiveness.

Acknowledgments The authors are grateful to Fundação de Amparo à Pesquisa do Estado de São Paulo (Fapesp 2008/56397-8 and 2008/58817-4).

References

Barth RF (2003) A critical assessment of boron neutron capture therapy: an overview. J Neurooncol 62:1–5

Barth RF, Matalka KZ, Bailey MQ, Staubus AE, Soloway AH, Moeschberger ML, Coderre JA, Rofstad EK (1994) A nude rat model for neutron capture therapy of human intracerebral melanoma. Int J Radiat Oncol Biol Phys 28:1079–1088

Cho HJ, Chun KJ, Park KW, Chung YS, Kim HR (2007) Determination of boron in a black mouse by prompt gamma activation analysis. J Radioanal Nuclear Chem 272:404–407

Coderre JA, Morris GM (1999) The radiation biology of boron neutron capture therapy. Radiat Res 151:1–18

Coderre JA, Glass JD, Fairchild RG, Micca PL, Joel DD (1990) Selective delivery of boron by the melanin precursor analogue boronophenylalanine in tumors other than melanoma. Cancer Res 50:138–141

Coderre JA, Slatkin DN, Micca PL, Ciallella JR (1991) Boron neutron capture therapy of a murine melanoma with p-boronophenylalanine: dose-response analysis using a morbidity index. Radiat Res 128:177–185

Coderre JA, Button TM, Micca PL, Fisher CD, Nawrocky MM, Liu HB (1994) Neutron capture therapy of the 9L rat gliosarcoma using the p-boronophenylalanine-fructose complex. Int J Radiat Oncol Biol Phys 30:643–652

Coelho PRP, Hernandes AC, Siqueira PTD (2002) Neutron flux calculation in a BNCT research facility implemented in IEA-R1 reactor. In: 10th International Congress on Neutron Capture Therapy. Research and development in neutron capture therapy. Wolfgang S, Raymond M, Andrea W. Essen, Germany (Bologna), pp 197–201

Dagrosa MA, Viaggi M, Rebagliati RJ, Batistoni D, Kahl SB, Juvenal GJ, Pisarev MA (2005) Biodistribution of boron compounds in an animal model of human undifferentiated thyroid cancer for boron neutron capture therapy. Mol Pharm 2:151–156

Faião-Flores F, Coelho PR, Arruda-Neto J, Maria DA (2011a) Boron neutron capture therapy induces cell cycle arrest and DNA fragmentation in murine melanoma cells. Appl Radiat Isot 69:1741–1744

Faião-Flores F, Coelho PR, Muniz RO, Souza GS, Arruda-Neto J, Maria DA (2011b) Antitumor potential induction and free radicals production in melanoma cells by Boron Neutron Capture Therapy. Appl Radiat Isot 69:1748–1751

Fernandez Y, Verhaegen M, Miller TP, Rush JL, Steiner P, Opipari AW Jr, Lowe SW, Soengas MS (2005) Differential regulation of noxa in normal melanocytes and melanoma cells by proteasome inhibition: therapeutic implications. Cancer Res 65:6294–6304

Fidler IJ (1975) Biological behavior of malignant melanoma cells correlated to their survival in vivo. Cancer Res 35:218–224

Fukuda H, Hiratsuka J, Honda C, Kobayashi T, Yoshino K, Karashima H, Takahashi J, Abe Y, Kanda K, Ichihashi M et al (1994) Boron neutron capture therapy of malignant melanoma using 10B-paraboronophenylalanine with special reference to evaluation of radiation dose and damage to the normal skin. Radiat Res 138:435–442

Gautier EA, Roberti MJ, Gettar RT, Jiménez Rebagliati R, Batistoni DA (2007) Assessment of chemical purity of 10B-enriched p-boronophenylalanine by high-performance liquid chromatography coupled on-line with inductively coupled plasma optical emission spectrometry. Anal Bioanal Chem 388:499–503

Gogas HJ, Kirkwood JM, Sondak VK (2009) Chemotherapy for metastatic melanoma: time for a change? Cancer 109:455–464

Ichikawa H, Taniguchi E, Fujimoto T, Fukumori Y (2009) Biodistribution of BPA and BSH after single, repeated and simultaneous administrations for neutron-capture therapy of cancer. Appl Radiat Isot 67:S111–S114

Ikeuchi I, Amano T (1978) A colorimetric determination of boron in biological materials. Chem Pharm Bull (Tokyo) 26:2619–2623

Jemal A, Siegel R, Ward E, Hao Y, Xu J, Thun MJ (2009) Cancer statistics, 2009. CA Cancer J Clin 59:225–249

Jiang G, Liu YQ, Wei ZP, Pei DS, Mao LJ, Zheng JN (2010) Enhanced anti-tumor activity by the combination of a conditionally replicating adenovirus mediated interleukin-24 and dacarbazine against melanoma cells via induction of apoptosis. Cancer Lett 294:220–228

Kamida A, Fujita Y, Kato I, Iwai S, Ono K, Suzuki M, Sakurai Y, Yura Y (2008) Effect of neutron capture therapy on the cell cycle of human squamous cell carcinoma cells. Int J Radiat Biol 84:191–199

Kreimann EL, Miura M, Itoiz ME, Heber E, Garavaglia RN, Batistoni D, Rebagliati RJ, Roberti MJ, Micca PL, Coderre JA, Schwint AE (2003) Biodistribution of a carborane-containing porphyrin as a targeting agent for boron neutron capture therapy of oral cancer in the hamster cheek pouch. Arch Oral Biol 48:223–232

Larrosa M, Tomás-Barberán FA, Espín JC (2003) Grape polyphenol resveratrol and the related molecule 4-hydroxystilbene induce growth inhibition, apoptosis, S-phase arrest, and upregulation of cyclins A, E, and B1 in human SK-Mel-28 melanoma cells. J Agric Food Chem 51:4576–4584

Mattiello EM, Ruiz HA, Silva IR, Sarkis JES (2011) Use of the HRICP-MS technique for the evaluation of boron isotopes in eucalitpus plants. Quím Nova 34:512–515

Mendes PF, Xander P, Novaes e Brito RR, Mortara RA, Jasiulionis MG, Lopes JD (2008) A cell surface 230 kDa protein from murine melanoma involved with tumor malignancy. Cancer Lett 262: 276–285

Menéndez PR, Roth BM, Pereira MD, Casal MR, González SJ, Feld DB, Santa Cruz GA, Kessler J, Longhino J, Blaumann H, Jiménez Rebagliati R, Calzetta Larrieu OA, Fernández C, Nievas SI, Liberman SJ (2009) BNCT for skin melanoma in extremities: updated Argentine clinical results. Appl Radiat Isot 67:S50–S53

Meyskens FL Jr (1981) Modulation of abnormal growth by retinoids: a clinical perspective of the biological phenomenon. Life Sci 28:2323–2327

Mishima Y, Honda C, Ichihashi M, Obara H, Hiratsuka J, Fukuda H (1989) Treatment of malignant melanoma by single thermal-neutron capture therapy with melanoma seeking B-10 compound. Lancet 2:388–389

Mosmann T (1983) Rapid colorimetric assay for cellular growth and survival: application to proliferation and cytotoxicity assays. J Immunol Methods 65:55–63

Probst TU (1999) Methods for boron analysis in boron neutron capture therapy (BNCT). A review. Fresenius J Anal Chem 364:391–403

Sauerwein W (1993) Principles and history of neutron capture therapy. Strahlenther Onkol 169:1–6

Soloway AH, Tjarks W, Barnum A, Rong FG, Barth RF, Codogni IM, Wilson JG (1998) The chemistry of neutron capture therapy. Chem Rev 98:1515–1562

Suzuki M, Nagata K, Masunaga S, Kinashi Y, Sakurai Y, Maruhashi A, Ono K (2004) Biodistribution of 10B in a rat liver tumor model following intra-arterial administration of sodium borocaptate (BSH)/degradable starch microspheres (DSM) emulsion. Appl Radiat Isot 61:933–937

Trivillin VA, Heber EM, Rao M, Cantarelli MA, Itoiz ME, Nigg DW, Calzetta O, Blaumann H, Longhino J, Schwint AE (2008) Boron neutron capture therapy (BNCT) for the treatment of spontaneous nasal planum squamous cell carcinoma in felines. Radiat Environ Biophys 47:147–155

Uchino H, Kanai Y, Kim DK, Wempe MF, Chairoungdua A, Morimoto E, Anders MW, Endou H (2002) Transport of amino acid-related compounds mediated by L-type amino acid transporter 1 (LAT1): insights into the mechanisms of substrate recognition. Mol Pharmacol 61:729–737

Wittig A, Michel J, Moss RL, Stecher-Rasmussen F, Arlinghaus HF, Bendel P, Mauri PL, Altieri S, Hilger R, Salvadori PA, Menichetti L, Zamenhof R, Sauerwein WA (2008a) Boron analysis and boron imaging in biological materials for Boron Neutron Capture Therapy (BNCT). Crit Rev Oncol Hematol 68(1):66–90

Wittig A, Malago M, Collette L, Huiskamp R, Buhrmann S, Nievaart V, Kaiser GM, Jockel KH, Schmid KW, Ortmann U, Sauerwein WA (2008b) Uptake of two 10B-compounds in liver metastases of colorectal adenocarcinoma for extracorporeal irradiation with boron neutron capture therapy (EORTC Trial 11001). Int J Cancer 122:1164–1171

Wittig A, Huiskamp R, Moss RL, Bet P, Kriegeskotte C, Scherag A, Hilken G, Sauerwein WA (2009) Biodistribution of (10)B for Boron Neutron Capture Therapy (BNCT) in a mouse model after injection of sodium mercaptoundecahydro-closo-dodecaborate and l-para-boronophenylalanine. Radiat Res 172:493–499

Yamamoto T, Nakai K, Matsumura A (2008) Boron neutron capture therapy for glioblastoma. Cancer Lett 262:143–152

Zhao W, Entschladen F, Liu H, Niggemann B, Fang Q, Zaenker KS, Han R (2003) Boswellic acid acetate induces differentiation and apoptosis in highly metastatic melanoma and fibrosarcoma cells. Cancer Detect Prev 27:67–75